

Title	Stress tensor of the hydrogen molecular ion
Author(s)	Ichikawa, Kazuhide; Tachibana, Akitomo
Citation	PHYSICAL REVIEW A (2009), 80(6)
Issue Date	2009-12
URL	http://hdl.handle.net/2433/109847
Right	© 2009 The American Physical Society
Type	Journal Article
Textversion	publisher

Stress tensor of the hydrogen molecular ion

Kazuhide Ichikawa and Akitomo Tachibana*

Department of Micro Engineering, Kyoto University, Kyoto 606-8501, Japan

(Received 19 August 2009; published 7 December 2009)

The electronic stress tensor of the hydrogen molecule ion H_2^+ is investigated for the ground state ($\sigma_g 1s$) and the first excited state ($\sigma_u^* 1s$) using their exact wave functions. A map of its largest eigenvalue and corresponding eigenvector is shown to be closely related to the nature of chemical bonding. For the ground state, we also show the spatial distribution of interaction energy density to describe in which part of the molecule stabilization and destabilization take place.

DOI: [10.1103/PhysRevA.80.062507](https://doi.org/10.1103/PhysRevA.80.062507)

PACS number(s): 31.10.+z, 31.15.ae, 03.65.-w

The stress tensors are used widely for description of internal forces of matter. They have been also established in quantum mechanical context [1], although it seems that basic idea dates back to Ref. [2]. Later, applications for quantum systems are investigated in many literatures from various aspects [3–22]. For example, Ref. [6] and followers have focused on stress tensor, which is associated with forces on nucleus. Our focus in this paper is electronic stress tensors, which measure effects caused by internal forces acting on electrons in molecules and particularly those between bonded atoms [12,15,16]. Such electronic stress tensor has been successfully used to define bond orders expressing the strength of chemical bonds [18]. It should be noted that people sometimes use different definitions for the stress tensor due to their own purpose and formalism. We use the expression derived by one of the authors in Ref. [12], which we believe most straightforward and suitable to discuss chemical bonds.

In this paper, we elucidate the role of the electronic stress tensor using hydrogen molecule ion H_2^+ , the simplest of all molecules, whose exact wave functions are known. Although there have been analyses of electronic stress tensor of other molecules using approximate wave functions expanded in the Gaussian functions [12,15,16,18,19,22], analysis using exact wave functions has not been conducted. We calculate spatial distributions of stress tensor and other associated quantities from the exact wave functions of H_2^+ and examine their detailed features that can be used to illustrate the chemical bond of the molecule. We believe that this paper demonstrates usefulness of the electronic stress tensor for an analysis of chemical bonding in the simplest but most exact form.¹

We begin by showing our expression of the electronic stress tensor τ_{ij}^S constructed from the H_2^+ wave function ψ . That is,

$$\tau_{ij}^S = \frac{\hbar^2}{4m} (\psi^* \partial_i \partial_j \psi - \partial_i \psi^* \partial_j \psi + \text{c.c.}), \quad (1)$$

where $\{i, j\} = \{1, 2, 3\}$ denote spatial coordinates, m is the electron mass, and c.c. stands for complex conjugate. The

expression for many-electron systems, that is, for almost every other molecule, is found in Ref. [12]. There, the stress tensor has been derived by field theoretic method which is applicable to many-particle system. Here, for illustrative purpose, we derive it using the Schrödinger equation for a single electron in H_2^+ .

The time-dependent Schrödinger equation reads

$$i\hbar \frac{\partial \psi}{\partial t} = -\frac{\hbar^2}{2m} \nabla^2 \psi + V\psi, \quad (2)$$

where the potential energy is assumed to be real. It is well-known that the continuity equation $\partial n / \partial t + \nabla \cdot \mathbf{j} = 0$ holds by defining probability density $n = |\psi|^2$ and probability flux $\mathbf{j} = (\hbar/m) \text{Im}(\psi^* \nabla \psi)$. Now, the equilibrium equation for electronic stress tensor is obtained from an equation of motion of \mathbf{j} . Namely, using Eq. (2), time derivative of \mathbf{j} can be written as

$$\frac{\partial \mathbf{j}}{\partial t} = -\frac{\hbar^2}{4m^2} (\nabla \psi \cdot \nabla^2 \psi^* - \psi^* \nabla \nabla^2 \psi + \text{c.c.}) - \frac{|\psi|^2}{m} \nabla V.$$

For the steady state, which is the case of molecular systems we consider, since $\partial \mathbf{j} / \partial t = 0$, we obtain the equilibrium equation

$$\partial_j \tau_{ij}^S + F_{L,i} = 0, \quad (3)$$

where $F_{L,i} = -|\psi|^2 \partial_i V$ is the Lorentz force generated by nuclei. For later convenience, we here define the first term in the equation as tension $F_{\tau,i} \equiv \partial_j \tau_{ij}^S$. From this equation, we see that τ_{ij}^S is the stress caused by purely quantum mechanical effect.

We compute the stress tensor defined by Eq. (1) using the exact wave functions of H_2^+ [25]. As is usually done for the stress tensor, we examine its largest eigenvalue and corresponding eigenvector. The sign of the largest eigenvalue tells whether electrons at a certain point in space feel tensile force (positive eigenvalue) or compressive force (negative eigenvalue) and the eigenvector tells direction of the force.

The case for the ground state ($\sigma_g 1s$) is plotted in the plane including two H nuclei as shown in the left panel of Fig. 1. The origin of the coordinate is taken to be the midpoint of the two nuclei. The eigenvalue along the internuclear axis is also plotted as red solid line in Fig. 2. The internuclear distance is taken to be 2.0 bohrs, which gives the equilibrium distance R_e (to be more precise, $R_e = 1.9972$ bohrs [26] but it

*akitomo@scl.kyoto-u.ac.jp

¹Calculations of stress tensor field as regards a H_2^+ molecule are found in Refs [23,24]. but with different definitions from ours.

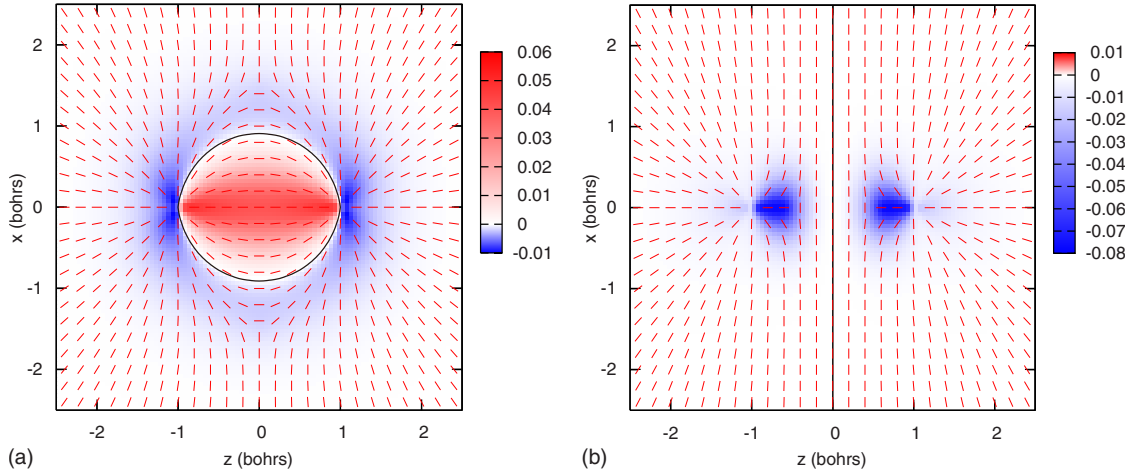


FIG. 1. (Color online) The spatial distributions of the largest eigenvalue and corresponding eigenvectors of stress tensor of H_2^+ molecule are plotted in the plane including two H nuclei. They are located at $(z, x) = (-1.0, 0.0)$ and $(1.0, 0.0)$. The left panel is for the ground state (σ_g^*1s) and the right panel is for the first excited state (σ_u^*1s). The black solid line shows the zero surface of the eigenvalue. For σ_g^*1s state, it is positive inside the circle and is negative outside. For the σ_u^*1s state, it is negative on both sides of the surface.

does not make practical difference in our argument below). The region with positive eigenvalue spreads between the nuclei, which corresponds to the formation of a chemical bond. The electronic stress tensor has this useful feature that it can express something is pulled up (that is, tensile force exists) when a covalent bond is formed. In detail, the positive eigenvalue region is bounded by a closed spherelike surface that touches two H nuclei. Also, in that region, the eigenvectors form a bundle of flow lines that connects the H nuclei. Such a region, called “spindle structure” [15], is clearly visible using the analysis with the exact wave function.

The case for the first excited state (σ_u^*1s) is shown in the right panel of Fig. 1 on the same plane and with the same internuclear distance. See also the green dashed line in Fig. 2 for the eigenvalue along the internuclear axis. Since this state does not form a bound state, we do not expect a bond between the H nuclei. Indeed, there is no region with positive

eigenvalue between the H nuclei for this case. In addition, eigenvectors are perpendicular to the internuclear axis at the region around the middle of the two H nuclei, showing there is no force connecting them.

These results, positive eigenvalue for bonding orbital and negative eigenvalue for antibonding orbital, are consistent with Ref. [15], where these features are pointed out using H_2 and He_2 , respectively.

We now examine the tension field $F_{\tau,i} \equiv \partial_j \tau_{ij}^S$ of the H_2^+ molecule. Writing explicitly,

$$\mathbf{F}_\tau = -\frac{\hbar^2}{4m} (\nabla \psi \cdot \nabla^2 \psi^* - \psi^* \nabla \nabla^2 \psi + \text{c.c.}). \quad (4)$$

Since this force, which cancels the classical Lorentz force at each point in space [Eq. (3)], also expresses purely quantum mechanical effects, it is considered to carry some information of a chemical bond. The spatial distribution of tension vector is plotted for σ_g^*1s and σ_u^*1s states in Fig. 3. On comparing Figs. 1 and 3, we see that in contrast with the case of the eigenvalue and eigenvector of the stress tensor, there is not much difference between the σ_g^*1s state and the σ_u^*1s state for the case of the tension vector. In Fig. 1, there is a striking difference between σ_g^*1s and σ_u^*1s that the former develops a region with positive eigenvalue while the latter exhibit negative region for the most of the space. There is also a marked difference in the pattern of eigenvectors at the internuclear region. In Fig. 3, the two states show a relatively similar pattern of the tension vector field. One difference can be pointed out that there is a point $(x, z) = (0.0, 0.0)$ at which tension vanishes for the σ_g^*1s state while the σ_u^*1s states has a plane $z=0$ on which it vanishes. However, overall feature resembles closely to each other. This indicates that the stress tensor has much more information as regards a chemical bond.

We note, however, that the tension can provide a handy way to characterize a chemical bond. Actually, it has been used to define an index of bond strength and turned out to be

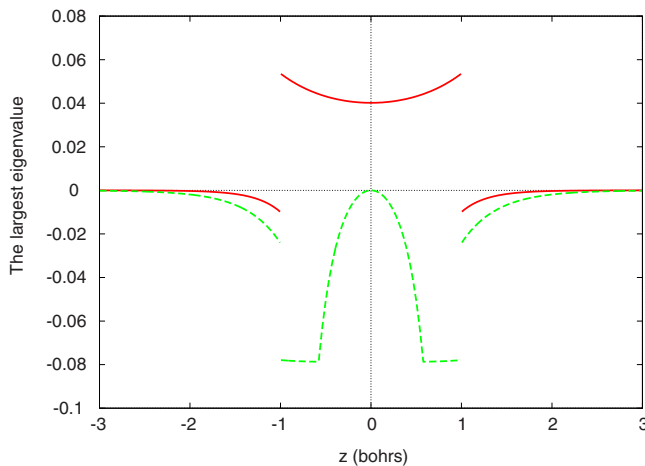


FIG. 2. (Color online) The largest eigenvalue of the stress tensor along the internuclear axis (along the z axis in Fig. 1). The red solid line is for the ground state (σ_g^*1s) and the green dashed line is for the first excited state (σ_u^*1s).

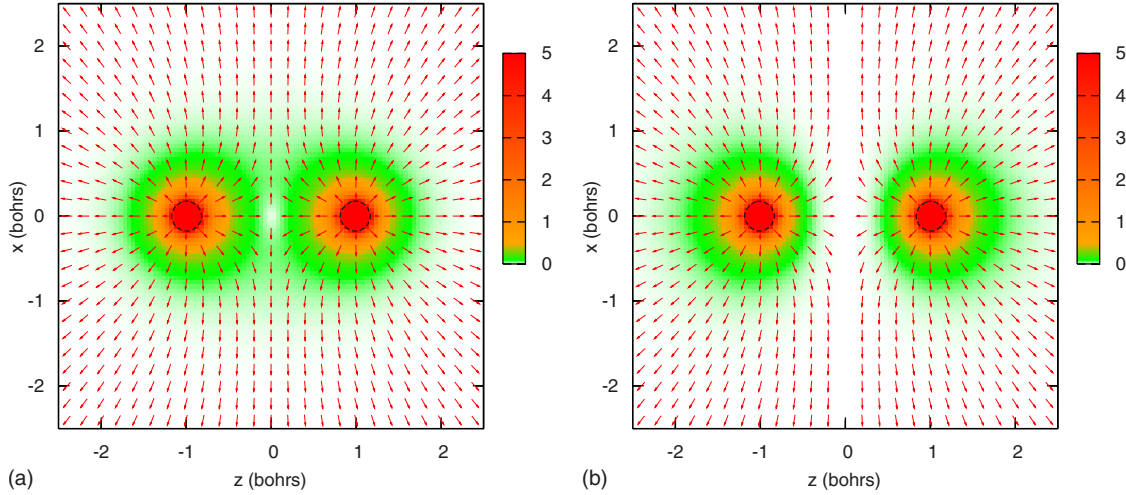


FIG. 3. (Color online) The spatial distributions of the tension \mathbf{F}_τ of H_2^+ molecule are plotted similarly to Fig. 1. The left panel is for the ground state (σ_g^*1s) and the right panel is for the first excited state (σ_u^*1s). Normalized tension vectors $\mathbf{F}_\tau/|\mathbf{F}_\tau|$ are shown by arrows and the norm $|\mathbf{F}_\tau|$ is depicted by a color map. $|\mathbf{F}_\tau|$ diverges at the positions of the nuclei. Contours which correspond to $|\mathbf{F}_\tau|=5$ are drawn by black dashed lines. $|\mathbf{F}_\tau|=0$ at $(0.0, 0.0)$ for the σ_g^*1s state and on $z=0$ for the σ_u^*1s state, where arrows are not shown.

very useful [18,19,22]. In Ref. [18], it has been proposed to calculate energy density [defined below, Eq. (6)] at the ‘‘Lagrange point,’’ which is defined as the vanishing point of the tension such as we have found at the midpoint of the internuclear axis of the ground state H_2^+ molecule in Fig. 3. It should also be noted that the existence of the Lagrange point alone cannot guarantee a chemical bond as is easily seen from the tension of the σ_u^*1s state of H_2^+ , which has the Lagrange point (or rather the Lagrange plane $z=0$). Hence, the tension can be a useful tool when combined with analysis of the stress tensor.

Finally, we describe our definition of energy density, which is derived from the stress tensor, and discuss the interaction energy density of the ground state of the H_2^+ molecule. In Ref. [12], it has been proposed to define energy density ε_τ from the trace of the stress tensor as

$$\varepsilon_\tau \equiv \frac{1}{2} \sum_i \tau_{ii}^s \quad (5)$$

$$= \frac{\hbar^2}{8m} (\psi^* \nabla^2 \psi - \nabla \psi^* \cdot \nabla \psi + \text{c.c.}). \quad (6)$$

Note that this definition gives correct total energy when integrated over the whole space and the virial theorem is applied. Furthermore, we consider the difference of the energy density between the ground state and the separated atoms. We call this interaction energy density $\Delta\varepsilon_\tau$ [18], and it is a useful quantity to discuss where in a molecule, stabilization or destabilization take place by chemical bond formation.

For the case of H_2^+ , it is appropriate to define $\Delta\varepsilon_\tau$ as

$$\Delta\varepsilon_\tau = \varepsilon_\tau(\text{H}_2^+) - \frac{\varepsilon_\tau(\text{H}_A) + \varepsilon_\tau(\text{H}_B)}{2}, \quad (7)$$

where H_A denotes the H atom at $z=-1.0$ and H_B at $z=1.0$ (as noted above, more precise R_e is 0.3% shorter and the virial theorem holds only at the equilibrium position but we can

practically consider R_e to be 2.0 bohrs). We plot this in the left panel of Fig. 4. From the definition, negative $\Delta\varepsilon_\tau$ [shown in blue (inside the solid line)] indicates stabilized regions and positive $\Delta\varepsilon_\tau$ [shown in red (outside the solid line)] indicates destabilized regions. We see that stabilization mostly takes place between the H nuclei. The stabilized region slightly expands outside of the internuclear region and the zero surface of $\Delta\varepsilon_\tau$ is found to include the two nuclei.

It is instructive to compare $\Delta\varepsilon_\tau$ with the differential electron density Δn ,

$$\Delta n = n(\text{H}_2^+) - \frac{n(\text{H}_A) + n(\text{H}_B)}{2}, \quad (8)$$

where $n=|\psi|^2$ is the ordinary electron density. This is plotted in the right panel of Fig. 4. We see that there is a region with increased electron density (shown in red) between the H nuclei and one with decreased electron density (shown in blue) outside the internuclear region. Compared with the map of $\Delta\varepsilon_\tau$, the region with increased electron density corresponds nicely to the stabilized region, which is consistent with a conventional picture of chemical bond formation. However, it should also be noticed that $\Delta\varepsilon_\tau$ and Δn do not have one-to-one correspondence. For example, we see in Fig. 4 that $\Delta\varepsilon_\tau$ has slightly larger zero surface than that of Δn . Moreover, integrating Δn over the whole space gives zero whereas $\Delta\varepsilon_\tau$ gives the difference of binding energy between H_2^+ and H atom.

In conclusion, we have calculated the stress tensor of the simplest molecule, H_2^+ , and demonstrated its relevance to chemical bonding. It is not only the simplest but is also most accurate due to the existence of the exact wave functions. By using them, we are able to investigate the eigenvalue and eigenvector of the stress tensor and the tension vector field of both the ground state and the first excited state in a very accurate manner. It also makes possible the precise comparison between the interaction energy density, which

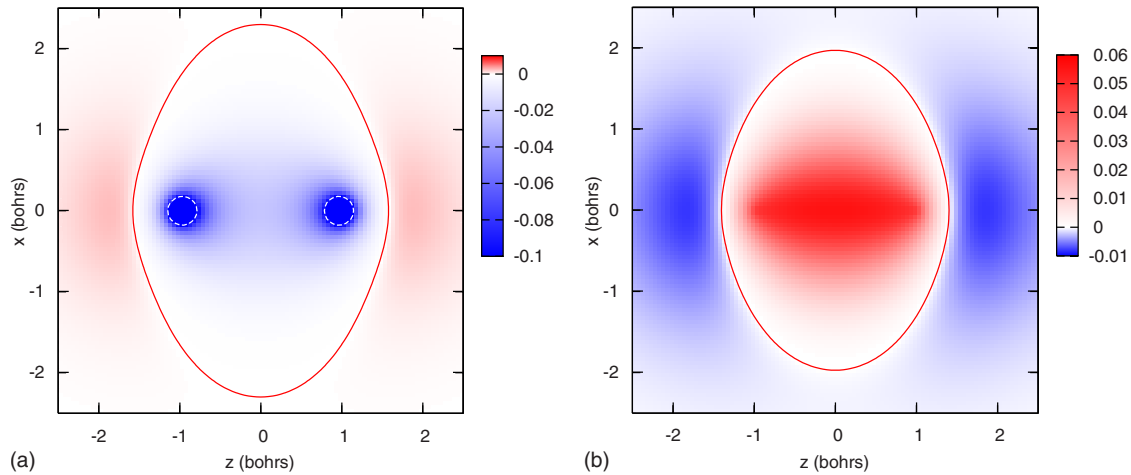


FIG. 4. (Color online) The spatial distributions of the interaction energy density $\Delta\epsilon_\tau$ (left panel) and the differential electron density Δn (right panel) of H_2^+ molecule are plotted for the ground state ($\sigma_g 1s$). The zero surface is shown by the red solid line for each panel. The interaction energy diverges at the positions of the nuclei and contours that correspond to $\epsilon_\tau = -0.1$ are shown by white dashed lines in the left panel.

tells the stabilized/destabilized regions, and conventional differential electron density with respect to the ground state. We believe that this calculation can be very useful as the most basic example which shows an important role of the electronic stress tensor for illustrating a chemical bond. Moreover, its exactness would serve as a benchmark to test validity of the calculation of the stress tensor which uses approximate wave functions. This is also very important

since we can only obtain approximate wave functions for almost every molecular system. Therefore, future investigation should include how the stress tensor of H_2^+ deviates from the exact form as we change the level of approximation of the quantum chemistry calculation to derive H_2^+ wave functions. Such a study will solidify the basis of the stress tensor analysis of molecular systems and open up areas of further application.

-
- [1] W. Pauli, *General Principles of Quantum Mechanics* (Springer-Verlag, New York, 1980).
- [2] E. Schrödinger, *Ann. Phys.* **386**, 109 (1926).
- [3] S. T. Epstein, *J. Chem. Phys.* **63**, 3573 (1975).
- [4] R. F. W. Bader, *J. Chem. Phys.* **73**, 2871 (1980).
- [5] A. S. Bamzai and B. M. Deb, *Rev. Mod. Phys.* **53**, 95 (1981).
- [6] O. H. Nielsen and R. M. Martin, *Phys. Rev. Lett.* **50**, 697 (1983).
- [7] O. H. Nielsen and R. M. Martin, *Phys. Rev. B* **32**, 3780 (1985).
- [8] N. O. Folland, *Phys. Rev. B* **34**, 8296 (1986).
- [9] N. O. Folland, *Phys. Rev. B* **34**, 8305 (1986).
- [10] M. J. Godfrey, *Phys. Rev. B* **37**, 10176 (1988).
- [11] A. Filippetti and V. Fiorentini, *Phys. Rev. B* **61**, 8433 (2000).
- [12] A. Tachibana, *J. Chem. Phys.* **115**, 3497 (2001).
- [13] A. Martín Pendás, *J. Chem. Phys.* **117**, 965 (2002).
- [14] C. L. Rogers and A. M. Rappe, *Phys. Rev. B* **65**, 224117 (2002).
- [15] A. Tachibana, *Int. J. Quantum Chem.* **100**, 981 (2004).
- [16] A. Tachibana, *J. Mol. Model.* **11**, 301 (2005).
- [17] S. Morante, G. C. Rossi, and M. Testa, *J. Chem. Phys.* **125**, 034101 (2006).
- [18] P. Szarek and A. Tachibana, *J. Mol. Model.* **13**, 651 (2007).
- [19] P. Szarek, Y. Sueda, and A. Tachibana, *J. Chem. Phys.* **129**, 094102 (2008).
- [20] J. Tao, G. Vignale, and I. V. Tokatly, *Phys. Rev. Lett.* **100**, 206405 (2008).
- [21] P. W. Ayers and S. Jenkins, *J. Chem. Phys.* **130**, 154104 (2009).
- [22] P. Szarek, K. Urakami, C. Zhou, H. Cheng, and A. Tachibana, *J. Chem. Phys.* **130**, 084111 (2009).
- [23] A. S. Bamzai and B. M. Deb, *Int. J. Quantum Chem.* **20**, 1315 (1981).
- [24] M. J. Godfrey, *J. Phys. B: At. Mol. Opt. Phys.* **23**, 2427 (1990).
- [25] D. R. Bates, K. Ledsham, and A. L. Stewart, *Philos. Trans. R. Soc. London, Ser. A* **246**, 215 (1953).
- [26] L. J. Schaad and W. V. Hicks, *J. Chem. Phys.* **53**, 851 (1970).